Int. J. Electrochem. Sci., 7 **(2012)** 11191 - 11205

International Journal of
ELECTROCHEMICAL
SCIENCE
www.electrochemsci.org

Electrochemical versus Ce(IV)-Mediated Electrochemical Oxidation (MEO) Degradation of Acetaminophen in Aqueous Solutions

Te-San Chen, Kuo-Lin Huang[*]*, Yi-Chuan Pan*

Department of Environmental Science and Engineering, National Pingtung University of Science and Technology, Pingtung 91201, Taiwan (ROC)
[*]E-mail: huangkL@mail.npust.edu.tw

Received: 24 September 2012 / *Accepted:* 11 October 2012 / *Published:* 1 November 2012

In this study, a lab-made PbO_2/Sn_2O_3-SnO_2/Ti electrode was compared with commercial boron doped diamond (BDD) and Pt anodes for Ce(IV) electro-regeneration and acetaminophen (AP) degradation. The Ce(IV) was electrochemically regenerated from Ce(III) in prepared and real spent Cr-etching solutions produced in TFT-LCD manufacturing processes. The regenerated Ce(IV) was used in a Ce(IV)-mediated electrochemical oxidation (MEO) process to compare with the anodes for AP degradation. The results show that 100% degradation of AP and *p*-benzoquinone (an intermediate of AP degradation) was achieved on all the tested electrodes in 30 min. The AP degradation performance of tested electrodes was in order BDD > PbO_2/Sn_2O_3-SnO_2/Ti > Pt, while the order changed to PbO_2/Sn_2O_3-SnO_2/Ti > Pt > BDD for Ce(IV) electro-regeneration. The degradation of AP by Ce(IV) oxidation increased with the increase of initial Ce(IV) concentration. When using Ce(IV) = 50 ppm regenerated from a real spent Cr-etching solution, the AP degradation efficiency was comparable to that of Ce(IV) = 200 ppm regenerated from prepared solutions. For 100% AP degradation, the PbO_2/Sn_2O_3-SnO_2/Ti and BDD electrodes required 15 min, but the Ce(IV) = 200 ppm case only needed 5 min. On the other hand, the degradation of AP-derived *p*-benzoquinone on PbO_2/Sn_2O_3-SnO_2/Ti reached 100% within 30 min, but that from Ce(IV) oxidation only increased slightly. Nevertheless, the abundant Ce(IV) regenerated from real spent Cr-etching solutions is a good candidate for being used in the MEO process for AP destruction. The prepared PbO_2/Sn_2O_3-SnO_2/Ti electrode is useful for both the electro-regeneration of Ce(IV) and the degradation of AP in aqueous solutions.

Keywords: Acetaminophen, Ce(IV)-mediated electrochemical oxidation, Ce(IV) electro-regeneration, Degradation.

1. INTRODUCTION

Recently, acetaminophen (AP) has received much attention because it is one of the most common pharmaceuticals found in households [1, 2] and is usually present in the effluent of sewage treatment plants and surface water [2–5]. In Taiwan, AP has been found to have high detection concentrations (the highest = 100,433 ng L^{-1}) (with a relatively high frequency of detection (over 90 %)) in water samples collected from different sources [1]. AP is also concerned for their adverse environmental effects [6].

Different methods have been reported for the destruction of AP, such as advanced oxidation processes (AOPs). One of the widely used AOPs is the Fenton method which uses hydrogen peroxide (H_2O_2) and ferrous ions (Fe^{2+}) in the generation of hydroxyl radicals which can degrade and mineralize a wide variety of pollutants [7–9]. However, the major disadvantage of Fenton process is the large production of ferric hydroxide sludge during the neutralization stage of the process. The removal efficiency of an AOP is generally a concern of researchers. A low AP removal efficiency (16.3%) was reported using a modified (photo) Fenton process [10]. In a study, ozonation and H_2O_2/UV, two other different AOPs, could only achieved partial mineralization of AP (30% and 40%, respectively) in the pH range 2.0–5.5 [11]. Thus, it is greatly in need to develop more reliable processes for the treatment of AP in water and wastewater.

During the past decade, electrochemical methods were proved to be efficient for destructing biologically persistent organic pollutants in water and wastewater; furthermore, total organic carbon (TOC) can be completely removed with high current efficiency [12]. Electrochemical techniques have various advantages such as wide application, simple equipment, easy operation, low temperature requirement, and no sludge formation [12, 13]. It is also attractive to use mediated electrochemical oxidation (MEO) processes for the destruction of organic pollutants because the oxidation reactions can be performed at ambient temperatures, the production of secondary waste is minimized, and organics may be completely mineralized to carbon dioxide and water, without emission of any toxic materials [14–18].

It is well known that the anode material plays an important role in the oxidation effectiveness, degradation pathway, and reaction mechanism of electrochemical destruction of organic pollutants. Nowadays, one of focuses on electro-oxidation technologies is the development of anode materials. Among electrode materials, PbO_2 is widely used as a metal oxide electrode due to its advantages such as low cost, effective oxidizing capacity, easy preparation, low electrical resistivity, relatively large surface area, and high oxygen evolution over-potential [19–21]. To the best of our knowledge, the Ce(IV) electrochemically regenerated in spent Cr-etching solutions generated from TFT-LCD manufacturing processes has not yet been used in MEO approaches. Also, the comparison of electrochemical and Ce(IV)-MEO degradation of AP is not available in the literature.

In this study, a PbO_2/Sn_2O_3-SnO_2/Ti electrode was fabricated, and then compared with commercial BDD and Pt anode materials for their performances of Ce(IV) regeneration (in terms of Ce(IV) yield and current efficiency) and AP oxidation. The Ce(IV) electrochemically regenerated in prepared and real spent Cr-etching solutions was used in a Ce(IV)-MEO process for AP oxidation. The

efficiencies of AP and AP-derived *p*-benzoquinone degradation in the Ce(IV)-MEO process was compared with those in the electrochemical approach.

2. MATERIALS AND METHODS

2.1. Chemicals and Materials

Cerium(III) nitrate hexahydrate, *p*-benzoquinone, and tin(II) chloride were obtained from Alfa Aesar (UK). Cerium(IV) Sulphate 4-hydrate was provided by Panreac Quimica (EU). Lead(II) nitrate, ammonium iron(II) sulfate hexahydrate, and sodium sulfate were from SHOWA Co. Ltd. (Japan). Aceton and acetonitrile were purchased from ECHO Chemical Co. Ltd. (Taiwan). Sulfuric acid (98%) and nitric acid (65%) (Scharlau, Spain) were used as received without further purification. Acetaminophen (AP) was purchased from Sigma (USA).

The stock solutions of AP (1000 mg L^{-1}) and *p*-benzoquinone were prepared by dissolving the chemicals into deionized distilled water (DDW), and then stored at 4^{o}C. The boron doped diamond (BDD) electrode was purchased from CONDIAS GmbH (Germany) (substrate: Niobium; BDD coating thickness: 2.0 mm).

2.2. Preparation of PbO_2/Sn_2O_3-SnO_2/Ti electrode

Commercially pure titanium plates were used as the substrate for the coating of tin oxides and lead dioxide. The titanium sheets (1.0 mm thickness, 99.5% purity) were mechanically polished using abrasive papers with successively finer roughness and then rinsed in two 15-min steps in ultrasonicated acetone and deionized distilled water (DDW). Acid pickling was done in a solution containing sulfuric acid 25% at 85^{o}C for 2 hr. The titanium sheets were dipped in a 0.5 M $SnCl_2$ solution at 85^{o}C for 2 hr to produce SnO_2 coating on the substrate and then the Ti plate is dried in a far-infrared drier for 15 min and followed by calcinations in muffle furnace at 400^{o}C for 60 min. Electro-deposition is employed for the preparation of PbO_2 coating on $SnCl_2$-treated titanium sheets. Experiments were conducted using a two-electrode electrochemical cell, in which the titanium sheet was used as the anode and a copper foil of similar size was used as the cathode. The gap between anode and cathode was fixed at 2 cm. The solution was agitated with a magnetic mixer at 200 rpm during the electroplating. The electroplating solution was made up of 0.5 M $Pb(NO_3)_2$, 0.1 M $Cu(NO_3)_2$, and 0.025 M NaF dissolved in 0.1 litter of DDW. Nitric acid was used to adjust the pH of electrolyte to be 1. The PbO_2 layer was generated in the above mentioned solution at 80 mA cm^{-2} for 40 min at 65^{o}C. A scanning electron microscope (SEM) (S-3000N, Hitachi, Japan) with energy-dispersive X-ray spectroscopy (EDS or EDX) (HORIBA EX-200) was used to examine the surface morphology and compositions of coatings on the prepared electrode, respectively. X-ray diffractometry (XRD) (Geigerflex 3063, with Ni-filtered Cu Kα radiation) was used for the analysis of specimen crystalline phases. The detector scanned over a range of angles (2θ) from 20^{o} to 80^{o}, at a step size of 0.01^{o} and a dwell time of 0.15 second per step (4^{o} (2θ) min^{-1}). The crystalline phases of tin and lead oxides were determined by comparing intensities and angles of peaks in the XRD patterns with those listed in the Joint Committee on Powder Diffraction

Standards (JCPDS) data files. Besides, the measurement of electrode electrochemical characteristic was performed using a CHI-660B potentiostat. A conventional three-electrode cell assembly consisting of the working electrode, an Ag/AgCl reference electrode, and a Pt wire counter electrode were used for the electrochemical measurements.

2.3. AP Electrolysis

The electro-oxidation of the AP aqueous solution was performed in a divided thermostatted cell. The anolyte (100 mL) was AP (10 ppm) in 4.8×10^{-4} M H_2SO_4 + 1 M Na_2SO_4 while the catholyte was only 4.8×10^{-4} M H_2SO_4 + 1 M Na_2SO_4. The anode and cathode compartments were separated by a Nafion 212 ion-exchange membrane separator. Prior to use, the Nafion 212 was heated at 65^{o}C in 1 M (~3%) H_2O_2 for 1 h to remove organic impurities. Then, the membranes were washed three times with DDW and stored in DDW.

The oxidation of aqueous AP was carried out under constant current density, temperature, and AP initial concentration. BDD, Pt, or PbO_2/Sn_2O_3-SnO_2/Ti was used as the anode whereas a stainless steel plate (SS 304) acted as the cathode for the electrolysis/degradation of AP. These anodes had the same geometric working surface areas (1cm^2). All the electrolytic experiments were performed using a DC power supply (Good Will Instrument CO., LTD GPS-2303). The cell voltage and current were monitored with time based on the readings of DC power supply. The anode potential was recorded using a digital multimeter which connected the anode with an Ag/AgCl reference electrode at a fixed location close to the anode.

Samples were taken at intervals during the electrolysis for 30 min. The concentrations of residual AP and AP-derived *p*-benzoquinone in samples were analyzed by a high performance liquid chromatography (HPLC) instrument (Hitachi chromaster 5420). The separations were performed on a RP-C18 column (250 mm×4.6 mm, particle size, 5μm). The mobile phase was acetonitrile/water (45:55, v/v), with a flow rate of 1mL min^{-1}. The injection volume was 20 μL and the working wavelength for quantitative analysis was 245 nm. The identification of each compound was based on the retention time of its standard. A personal computer equipped with a Hitachi chromaster system manager for LC systems was used to acquire and process chromatographic data.

2.4. Ce(IV) electro-regeneration

The Ce(IV) electro-regeneration was carried out using a divided electrochemical cell under constant current density. The anode and cathode compartments were separated by an ion-exchange membrane separator (AMI-7001). Both electrolytic cells used a BDD, Pt, or PbO_2/Sn_2O_3-SnO_2/Ti electrode as the anode and a stainless steel plate (SS 304) as the cathode (1 cm^2). The anolyte (100 mL) was 0.2 M Ce(III) in 4 M HNO_3 while the catholyte was only 4 M HNO_3. For the Ce(IV) electro-generated from a real spent Cr-etching solution, both anolyte (100 mL) and catholyte (100 mL) were real spent Cr-etching solutions. All the electrolytic experiments were performed under constant current electrolysis using a DC power supply (Good Will Instrument CO., LTD GPS-2303) at constant

temperature (25^{o}C). The cell voltage and current were monitored with time based on the readings of DC power supply. The anode potentials were recorded using a digital multimeter which connected the anode with an Ag/AgCl reference electrode at a fixed location close to the anode.

Samples were taken at intervals during the electrolysis for 240 min. A redox potential titrator (Metrohm 702 SM Titrino) was used to quantitatively determine the Ce(IV) concentrations of samples by ferrous ammonium sulfate dissolved in 1 M nitric acid [22]. The concentrations of total cerium were analyzed by inductively couple plasma atomic emission spectrometry (ICP-AES) (Perkin Elmer optima 2100 DV).

The theoretical production of Ce(IV) amount (m_t) at electrolysis time t can be calculated as follows [23].

$$m_t = MIt/zF \quad (1)$$

where M: molecular weight of Ce, I: current, z: electrons transferred per Ce(III) ion (z = 1 in Ce(III) → Ce(IV) + e^-), and F: the Faraday's constant. The current efficiency is calculated based on the following equation

$$\text{Current efficiency (CE)} = (m_e/m_t)\times 100\% \quad (2)$$

where m_e is the Ce (IV) amount obtained experimentally. The Ce(IV) percent yield is calculated using

$$\text{Yield (\%)} = (C_e(IV)_A/C_e(IV)_T)\times 100\% \quad (3)$$

where $Ce(IV)_A$ is the actual amount of Ce(IV) generated in electrolysis for a period of time and $Ce(IV)_T$ is the theoretical amount of Ce(IV) that can be generated. In this study, $Ce(IV)_T$ = Electrolyte volume × ($[Ce(III)]_{initial}$ + $[Ce(IV)]_{initial}$) = Electrolyte volume × ($[Ce(III)]_{initial}$) because the $[Ce(IV)]_{initial}$ = 0.

2.5. Ce(IV)-MEO degradation of AP

The batch Ce(IV)-MEO degradation studies were carried out by adding different amount of Ce(IV) into 100 mL solution which initially contained 10 ppm AP in an undivided reactor. The solution was thoroughly mixed by a magnetic stirrer and tested under room temperature. Samples were taken at intervals with immediate addition of excess ferrous ions during the degradation of AP by Ce(IV) oxidation to prevent the AP from subsequent oxidation by residual Ce(IV). Again, the concentrations of residual AP and AP-derived *p*-benzoquinone in samples were analyzed by the HPLC analyzer (Hitachi chromaster 5420).

3. RESULTS AND DISCUSSION

3.1. Characterization of the prepared PbO_2/Sn_2O_3-SnO_2/Ti electrodes

Figure 1 shows the XRD patterns of crystalline phases of metal oxides.

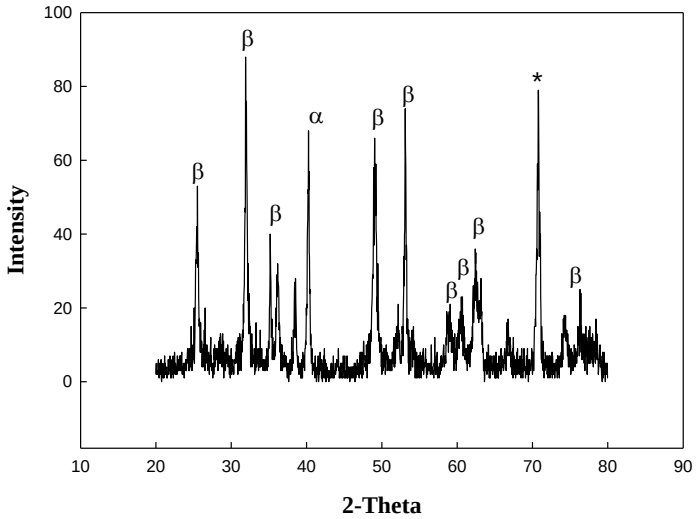

Figure 1. XRD patterns of crystalline phases of lead and tin oxides.

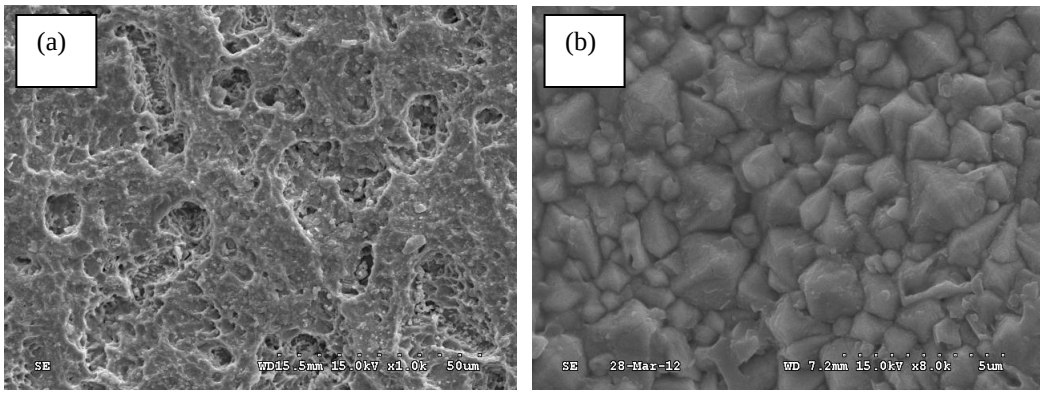

Figure 2. SEM images of the electrode surfaces of (a) Sn_2O_3-SnO_2/Ti, (b) PbO_2/Sn_2O_3-SnO_2/Ti.

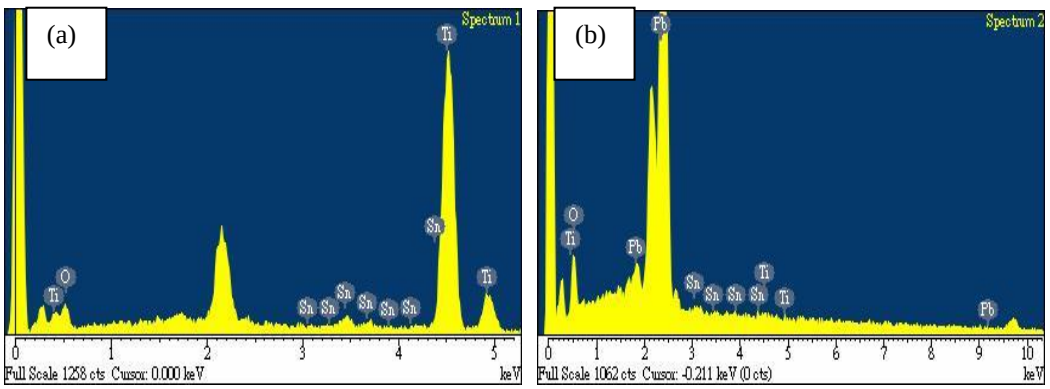

Figure 3. EDS analysis of the coating surfaces of (a) Sn_2O_3-SnO_2/Ti, (b) PbO_2/Sn_2O_3-SnO_2/Ti.

Obviously, the PbO_2 crystalline phases were dominated by β-PbO_2 which was preferred when PbO_2 was used as electrode material because the conductivity is greater for β-PbO_2 than for α-PbO_2 [24]. The peak at $2\theta = 71^o$ (asterisk-marked) possibly refers to that of Ti, SnO_2, or Sn_2O_3, because the XRD analysis is not straightforward, due to the superposition of different diffraction peaks corresponding to mixtures of Sn_2O_3-SnO_2/Ti. The surface of Sn_2O_3-SnO_2 layer chemically deposited on the Ti plat exhibited a layered texture (Figure 2(a)),whereas that of PbO_2 film on the Sn_2O_3-SnO_2/Ti had a relatively homogeneous appearance (Figure 2(b)), corresponding to the tetragonal morphology of β-PbO_2 [24, 25] and supporting the result of XRD analysis. It was also observed that the β-PbO_2 layer could well cover the Sn_2O_3-SnO_2 layer. The β-PbO_2 layer consisted of tightly packed and angular crystals. The average size of the β-PbO_2 crystals was about 1 μm. Despite of the large crystal size of the surface β-PbO_2 layer, no obvious cracks were observed. This is helpful for improving the electrode stability [25]. The EDS analyses of Sn_2O_3-SnO_2/Ti and PbO_2/Sn_2O_3-SnO_2/Ti shown in Figure 3 also support the observation of SEM.

3.2. Effect of anode material on Ce(IV) electro-regeneration

In this study, the prepared PbO_2/Sn_2O_3-SnO_2/Ti electrode and two commercial available anode materials (Pt and BDD) were tested and compared for their performance on Ce(III) oxidation. In general, the Ce(IV) yield is associated with the operating anode potential and Ce(III) oxidation potential, while the current efficiency (CE) is also related to the oxygen evolution potential on electrode. At 0.15 A cm^{-2}, the performance of anodes for Ce(IV) electro-regeneration was in order PbO_2/Sn_2O_3-SnO_2/Ti > Pt > BDD in terms of Ce(IV) yield and CE in 4 M HNO_3 (Figure 4), consistent with their operating anode potentials but inconsistent with their oxygen evolution potentials (typically BDD > PbO_2 ≥ Pt (Figure 5)).

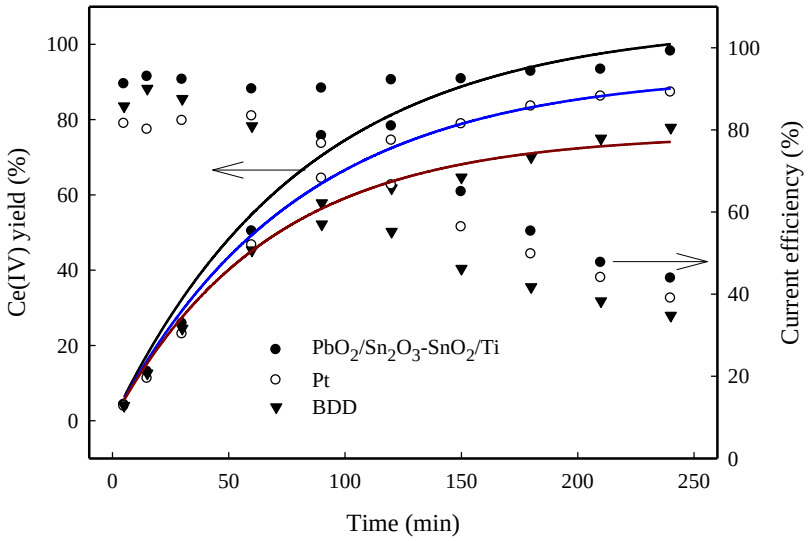

Figure 4. Effect of anode material on current efficiency and Ce(IV) yield in the divided cell (anolyte: 0.2 M Ce(III) in 4 M HNO_3, catholyte: 4 M HNO_3, separator: AMI-7001, anode: 2 cm^2, stainless steel cathode: 1 cm^2, and I = 0.3 A).

According to the CV measurements of these three electrode in 4 M HNO_3 containing 0.1 M Ce(III), although the redox peak currents of Ce(IV)/Ce(III) were greater on BDD than on Pt, the Ce(III) oxidation peak potentials for BDD and Pt were 1.746 and 1.591 V, respectively; the formal potential (average of redox peak potentials) of Ce(III)/Ce(IV) was more positive on BDD (1.42 V) than on Pt (1.30 V), while the peaks of Ce(IV)/Ce(III) redox reactions could not be clearly identified for PbO_2/Sn_2O_3-SnO_2/Ti (Figure 5). The apparent rate constants for Ce(III) oxidation on the PbO_2/Sn_2O_3-SnO_2/Ti, Pt, and BDD anodes were 2.31×10^{-4}, 1.77×10^{-4}, and 1.29×10^{-4} s^{-1}, respectively, with corresponding apparent mass transfer coefficients of 1.15×10^{-2}, 7.86×10^{-3}, and 6.64×10^{-3} cm s^{-1}, respectively. For the Ce(III) oxidation at 0.88 A cm^{-2} in the real spent Cr-etching solution on PbO_2/Sn_2O_3-SnO_2/Ti, the Ce(IV) yield at 150 min was over 90%, and reached 100% at 240 min (Figure 6); therefore, the PbO_2/Sn_2O_3-SnO_2/Ti anode is suitable for Ce(IV) electro-regeneration in real spent Cr-etching solutions (pH < 0).

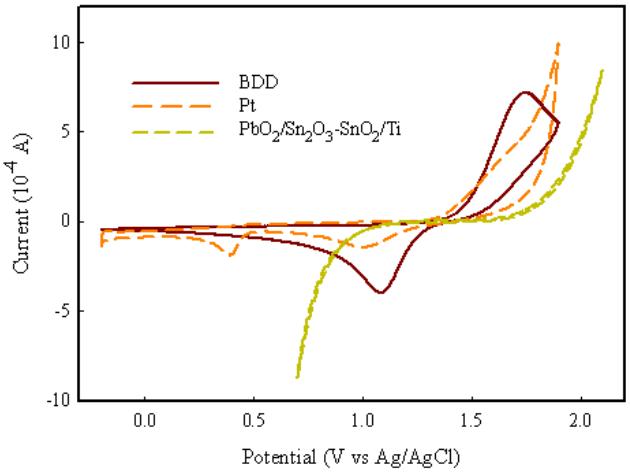

Figure 5. Cyclic voltammograms of 0.1 M Ce(III) in 4 M HNO_3 for tested electrodes (scan rate = 100 mV s^{-1}).

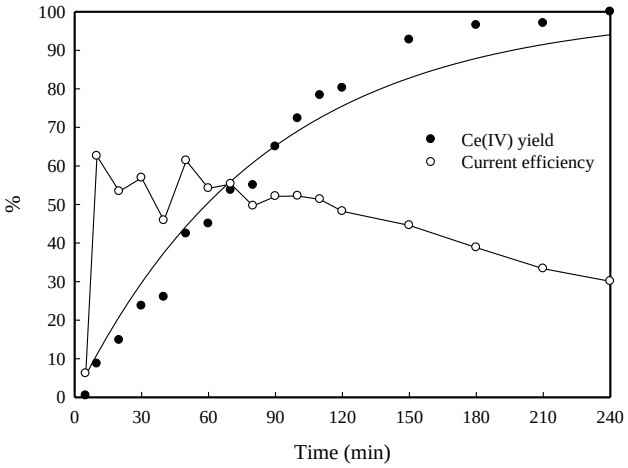

Figure 6. Ce(IV) regeneration in the real spent Cr-etching solution (Ce(III): 0.39 M, separator: AMI-7001, PbO_2/Sn_2O_3-SnO_2/Ti anode: 1 cm^2, stainless steel cathode: 1 cm^2, and I = 0.88 A).

3.3. Electrochemical characterization of AP and p-benzoquinone on tested anode materials

The electrochemical properties of AP at different anode materials were investigated using cyclic voltammetry in 1 M Na_2SO_4 solutions. Figures 7a to d show the cyclic voltammograms (CV) recorded at a sweep rate of 100 mV s^{-1} in 100 ppm AP solutions for different tested electrodes. (The potential reported hereafter for CV analysis are all vs. Ag/AgCl.) The CV tests were performed initially using a glassy carbon (GC) electrode to verify the peaks of AP oxidation and vice-versa. On the GC electrode, the voltammogram of AP shows an oxidation peak and a corresponding reduction peak at 0.557 and 0.460 V, respectively (Figure 7a); the anodic and cathodic peaks correspond to the conversion of AP to *N*-acetyl-*p*-benzoquinone-imine (NAPQI) and vice-versa [26, 27]. This phenomenon was also observed on Pt, but its peak potential separation was greater than that on GC (Figure 7b).

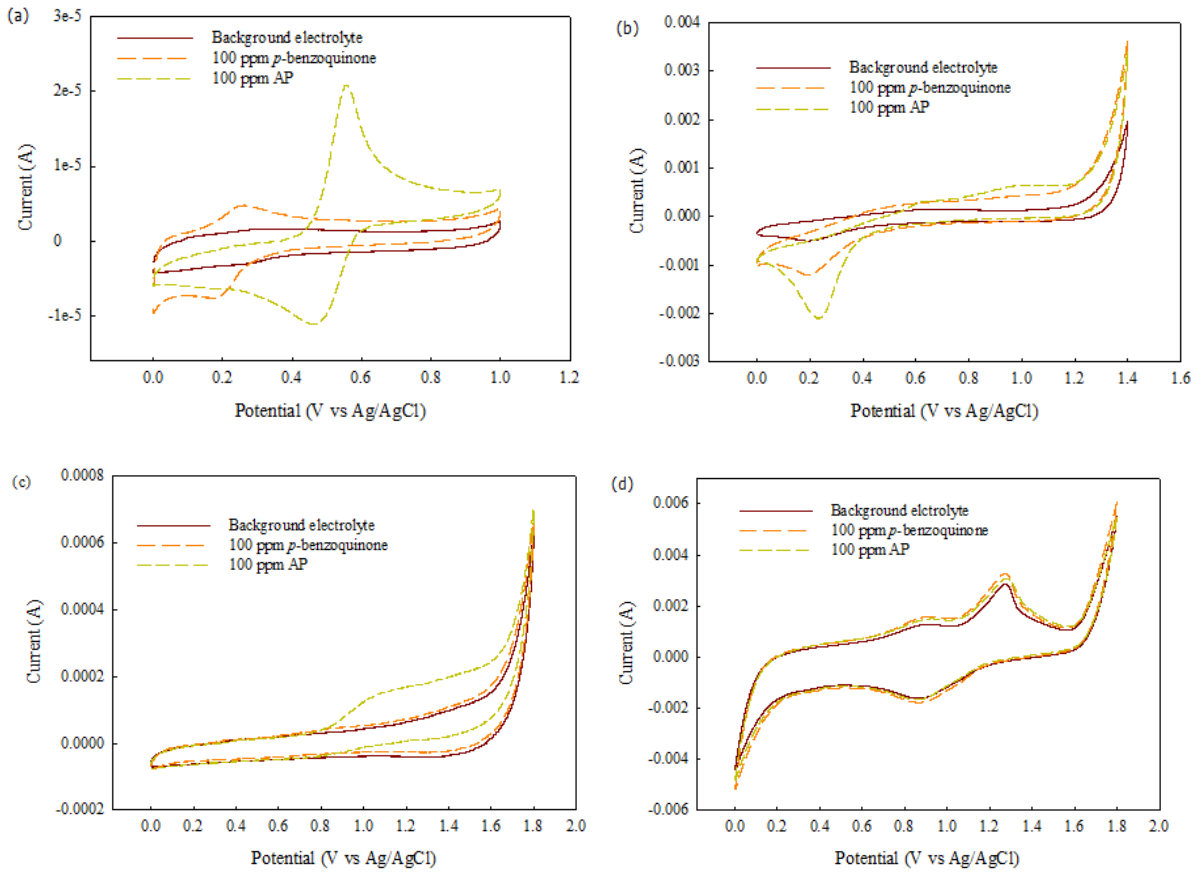

Figure 7. Cyclic voltammograms of 100 ppm AP, 100 ppm *p*-benzoquinone and background electrolyte (1 M Na_2SO_4) for tested electrodes (scan rate = 100 mV s^{-1}) (a) GC, (b) Pt, (c) BDD and (d) PbO_2/Sn_2O_3-SnO_2/Ti.

Although the oxidation peak of AP appeared in the CV of BDD, its corresponding reduction peak could not be clearly identified (Figure 7c). For the CV of prepared electrode (PbO_2/Sn_2O_3-SnO_2/Ti), no peak of AP oxidation was seen in the working potential window, because when using the

solution containing AP, the oxidation and reduction peaks displayed in Figure 7d were all similar to those (possibly corresponding to the oxidation and reduction of Pb(IV)/Pb(II)/Pb(0) couples [28]) for the background electrolyte.

P-benzoquinone is one of important intermediates that may be formed in the process of AP electro-oxidation (see more discussion in section 3.6). Therefore, the electrochemical characteristics of *p*-benzoquinone at different anode materials were also investigated using CV in 1 M Na_2SO_4 solutions. Again, the CV of GC shows the peaks of *p*-benzoquinone oxidation and corresponding reduction at 0.263 and 0.168 V, respectively (Figure 7a), reflecting the transformation of *p*-benzoquinone to lower aliphatic acids and vice-versa [29]. However, the peak potential separation was greater on Pt than on GC (Figure 7b). On both BDD and PbO_2/Sn_2O_3-SnO_2/Ti, no peak of *p*-benzoquinone oxidation was observed in the working potential window (Figures 7c and d). (Note that the oxidation and reduction peaks displayed in Figure 7d when using the solution containing *p*-benzoquinone were all similar to those of the background electrolyte.)

3.4. Effect of anode material on AP degradation

It is well known that the anodic oxidation of organics is strongly dependent on anode material. In this study, Pt, PbO_2/Sn_2O_3-SnO_2/Ti, and BDD anodes were tested to compare their performance in AP electro-oxidation/degradation at a galvanostatic condition (500 mA cm^{-2}) (initial AP concentration = 10 ppm). As shown in Figure 8, the abatement of the AP obtained by anodic oxidation dramatically depends on the nature of the anode material. After 6 min constant current electrolysis, no residual AP was detected (AP degradation efficiency = $(1-(C/C_o))\times100$ = 100%) when BDD was used as the anode. At the same electrolysis time, however, the degradation efficiency of AP was only about 50 % on the Pt or PbO_2/Sn_2O_3-SnO_2/Ti anode. To achieve 100% AP degradation, the Pt and PbO_2/Sn_2O_3-SnO_2/Ti anodes needed 15 min. This phenomenon is attributed chiefly to anode potential and hydroxyl radical (·OH) associated with the direct anodic oxidation of AP.

During electrolysis, the magnitude of anode potentials of tested electrodes followed the order BDD > PbO_2/Sn_2O_3-SnO_2/Ti > Pt. A higher anodic potential may generate a greater electron trapping activity, favorable to organic oxidation [30] and ·OH production (from water electrolysis) [31] on the anode surface. Accordingly, the magnitude of acetaminophen (AP) degradation efficiency was in order BDD > PbO_2/Sn_2O_3-SnO_2/Ti > Pt. BDD was also reported to be better than Pt in the electrochemical degradation of bisphenol A [32]. Some researchers also indicated that BDD electrodes were superior to Pt and PbO_2 anodes for the electro-oxidation of bisphenol A [33, 34]. Furthermore, the regressions of AP degradation data were all linear (the inset of Figure 8), revealing that the AP degradation kinetics could be regarded as pseudo-first-order. The apparent rate constants were 8.06×10^{-3}, 1.94×10^{-3}, and 1.59×10^{-3} s^{-1} at BDD, PbO_2/Sn_2O_3-SnO_2/Ti, and Pt, respectively. On the other hand, the potentials of oxygen evolution were similar on BDD and PbO_2/Sn_2O_3-SnO_2/Ti, ~1.6 V vs. Ag/AgCl, which was about 0.3 V higher than that on Pt (Figure 7), suggesting that the current efficiency of AP degradation was greater on BDD or PbO_2/Sn_2O_3-SnO_2/Ti than on Pt.

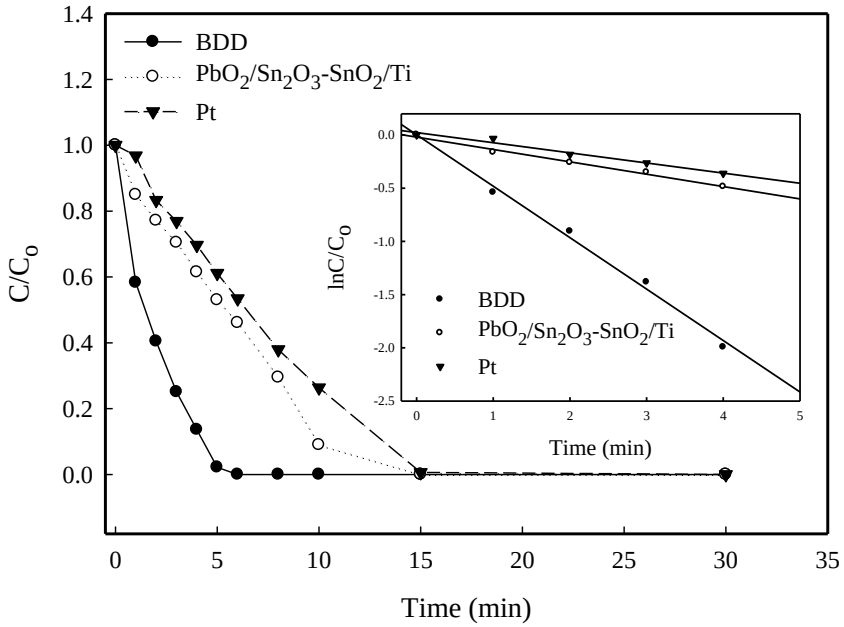

Figure 8. Variation of AP C/C_o with time for tested anodes (surface area =1 cm^2) at 0.5 A ($[AP]_o$ = 10 ppm, electrolyte: 4.8×10^{-4} M H_2SO_4 + 1 M Na_2SO_4, temperature = 25 ^oC, and cathode: Ti 1cm^2); inset: $\ln(C/C_o)$ against time.

3.5. Ce(IV)-MEO degradation of AP

For comparison, the degradation of AP was also carried out in a simple undivided type reactor by a mediated electrochemical oxidation (MEO) process using the Ce(IV) mediators regenerated from prepared and real spent Cr-etching solutions. When using regenerated Ce(IV) = 10 ppm from the prepared solution, the degradation of AP was fast during the initial 1 min, slower within 1−5 min, and then almost negligible from 5 to 30 min; however, the AP degradation efficiencies of 1, 5, and 30 min were only 40.2%, 49.4%, and 51.7%, respectively (Figure 9). Similar trends of AP degradation were found when increasing initial Ce(IV) concentration, but the AP degradation efficiency was noticeably improved. For Ce(IV) = 50 ppm, the 1, 5, and 30 min AP degradation efficiencies reached 77.1%, 89.8%, and 98.3%, respectively; at Ce(IV) = 100 ppm, the corresponding values were 90.6%, 93.8%, and 98.6%, respectively. For Ce(IV) = 200 ppm, the AP degradation efficiency achieved 99.1% at 1 min and 100% at 5 min. This behavior of AP degradation by Ce(IV) oxidation is similar to those of organics degradation by Ce(IV) or other mediators in MEO processes [14, 35]. At the point of quick AP degradation in short time and for simplification, the apparent rate constants obtained from the regressions of AP degradation data were 2.48×10^{-3}–3.62×10^{-2} s^{-1} (increasing with the increase of initial Ce(IV) concentration), assuming that these reactions were all pseudo-first-order.

When using Ce(IV) = 50 ppm regenerated from the real spent Cr-etching solution, the 1, 5, and 30 min AP degradation efficiencies were 90.6%, 93.8%, and 98.6%, respectively; these data were in between those of Ce(IV) = 100 and 200 ppm, and noticeably higher than those of Ce(IV) = 50 ppm regenerated from the prepared solution (Figure 9). This phenomenon is related to the fact that the real

spent Cr-etching solution contained other oxidizing species such as $Cr_2O_7^{2-}$ (0.27 M) and NO_3^- (8.36 M) [36] which resulted in additional degradation of AP. Therefore, although the pseudo-first-order apparent rate constant of this case was 3.62×10^{-2} s^{-1}, its reaction is more complicated and further study is necessary to identify the reaction order.

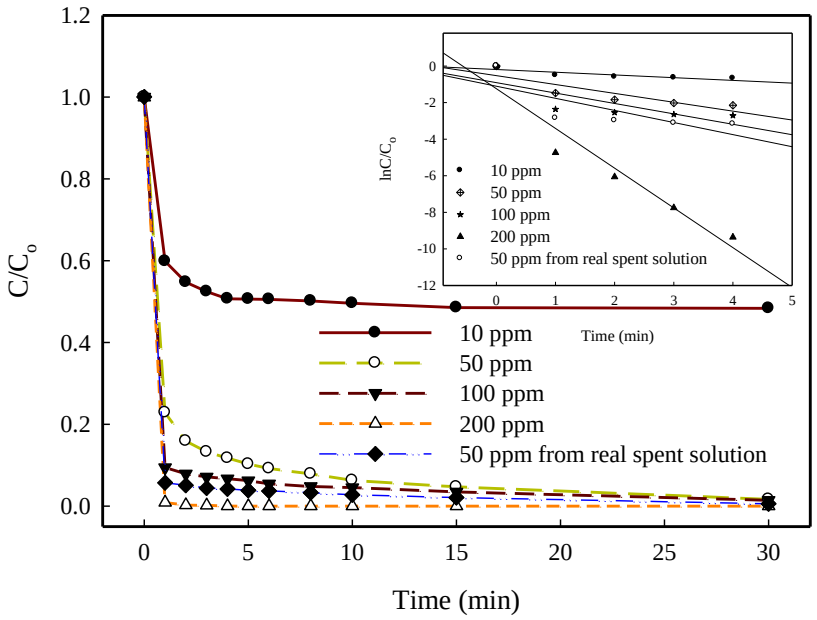

Figure 9. Effect of Ce(IV) concentration on AP degradation ($[AP]_o$= 10 ppm); inset: $\ln(C/C_o)$ against time).

Nevertheless, the result shows that it is optimistic to use the regenerated real spent Cr-etching solution containing abundant Ce(IV) (0.39 M) [36] in the Ce(IV)-MEO process for AP destruction.

3.6. Electrochemical vs Ce(IV)-MEO degradation of AP

In general, the AP degradation was faster by Ce(IV) oxidation than by electro-oxidation in this study, particularly for that at reaction time ≤5 min. At 1 and 5 min, the AP degradation efficiencies were 15.0% and 47%, respectively, on PbO_2/Sn_2O_3-SnO_2/Ti, and 3.2% and 38.9%, respectively, on Pt, significantly lower than those of Ce(IV) = 10 ppm case (40.2% and 49.4%, respectively). The AP degradation efficiency of BDD at 1 min (41.7%) was also significantly lower than that of Ce(IV) = 50 ppm case (77.1%). The time required for 100% AP degradation at Ce(IV) = 200 ppm (5 min) was only one-third that at PbO_2/Sn_2O_3-SnO_2/Ti and BDD electrodes (15 min). On the other hand, the degradation of *p*-benzoquinone (an intermediate from AP electro-degradation) on PbO_2/Sn_2O_3-SnO_2/Ti reached 100% within 30 min (Figure 10(a)), but that from Ce(IV) oxidation only increased slightly in the same time period (Figure 10(b)). (Note that the peaks at retention time = ~2.3 min might be referred to intermediates (e.g., lower aliphatic acids [29])) from *p*-benzoquinone oxidation, because the variation of these peaks was opposed to that of *p*-benzoquinone. Therefore, further study is necessary to try if more degradation of *p*-benzoquinone can be achieved using the Ce(IV)-MEO approach.

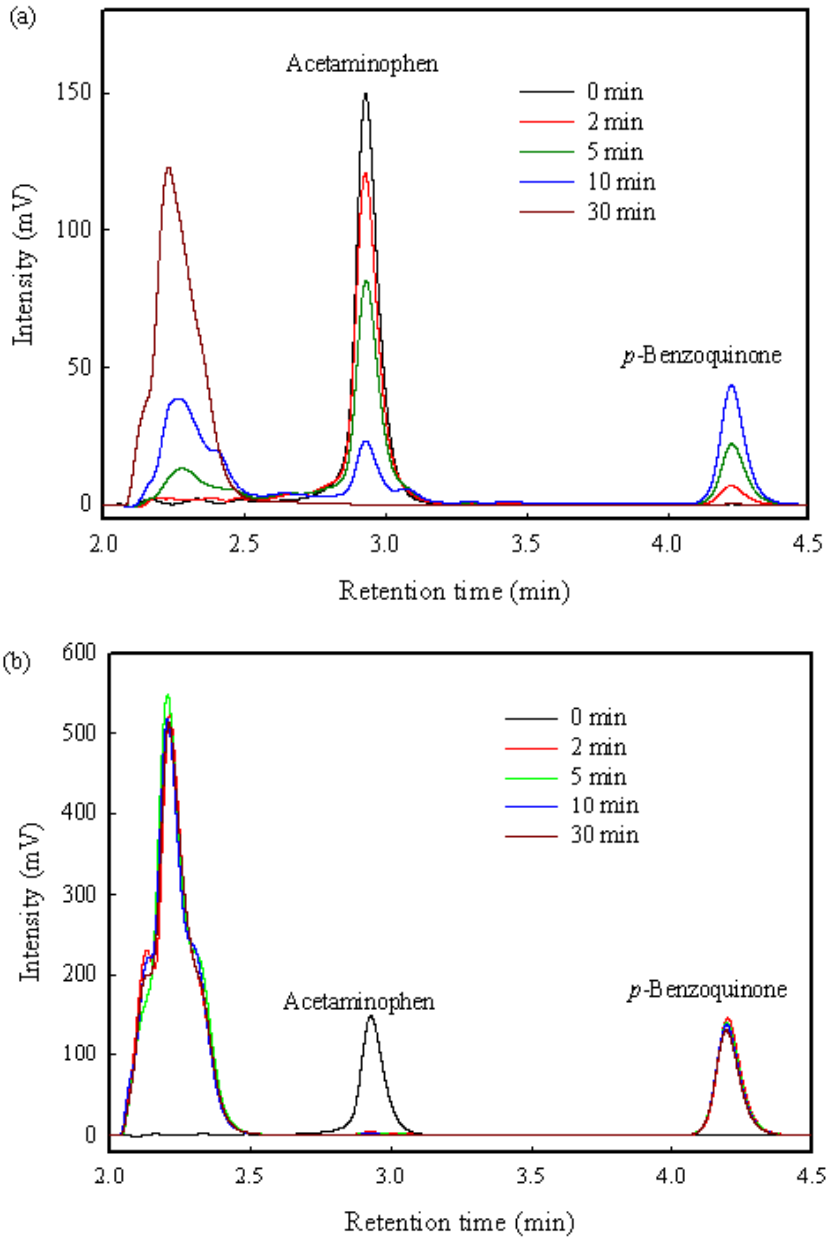

Figure 10. LC chromatograms for acetaminophen degradation: (a) electro-oxidation on PbO_2/Sn_2O_3-SnO_2/Ti electrode; (b) Ce(IV)-MEO at 200 ppm Ce(IV) ($[AP]_o$ = 10 ppm).

4. CONCLUSIONS

In this study, the performance of anodes for Ce(IV) electro-regeneration was in order PbO_2/Sn_2O_3-SnO_2/Ti > Pt > BDD in terms of Ce(IV) yield and CE in 4 M HNO_3. AP can be completely removed using the tested anodes and its kinetics follows a pseudo-first-order reaction. The apparent rate constants for Ce(III) oxidation on the PbO_2/Sn_2O_3-SnO_2/Ti, Pt, and BDD anodes were 2.31×10^{-4}, 1.77×10^{-4}, and 1.29×10^{-4} s^{-1}, respectively, with corresponding apparent mass transfer

coefficients of 1.15×10^{-2}, 7.86×10^{-3}, and 6.64×10^{-3} cm s^{-1}, respectively. The Ce(IV) yield reached 100% at 240 min when using PbO_2/Sn_2O_3-SnO_2/Ti in both the prepared and real spent Cr-etching solutions. On Pt and BDD, the peaks of AP oxidation could be observed in CV analysis, but those of *p*-benzoquinone (an intermediate from AP degradation) oxidation were not so clearly shown within the working potential window.

The magnitude of AP degradation efficiency was in order BDD > PbO_2/Sn_2O_3-SnO_2/Ti > Pt. The pseudo-first-order apparent rate constants of AP electro-degradation were 8.06×10^{-3}, 1.94×10^{-3}, and 1.59×10^{-3} s^{-1} at BDD, PbO_2/Sn_2O_3-SnO_2/Ti, and Pt, respectively, while those by (prepared) Ce(IV) oxidation were in the range 2.48×10^{-3}–3.62×10^{-2} s^{-1}, increasing with the increase of initial Ce(IV) concentration (50−200 ppm). When using Ce(IV) = 50 ppm regenerated from a real spent Cr-etching solution, the AP degradation efficiency was comparable to those of Ce(IV) = 200 ppm regenerated from the prepared solution.

Although the AP degradation was faster by Ce(IV) oxidation in the Ce(IV)-MEO process than by electro-oxidation, particularly for that in the initial stage of reaction (≤5 min), the degradation of *p*-benzoquinone on PbO_2/Sn_2O_3-SnO_2/Ti reached 100% within 30 min while that from Ce(IV) oxidation at Ce(IV) = 200 ppm only increased slightly in the same time period. Nevertheless, the Ce(IV) regenerated in real spent Cr-etching solutions is a good candidate to be used in the Ce(IV)-MEO process for AP destruction. The prepared PbO_2/Sn_2O_3-SnO_2/Ti electrode is suitable for the electro-regeneration of Ce(IV) in real spent Cr-etching solutions and the degradation of AP in aqueous solutions. Both techniques tested in this study have a good potential to be applied for organic pollutant destruction in aqueous solutions.

ACKNOWLEDGMENTS

The authors thank the National Science Council of Taiwan for financial support of this research under contract nos. NSC−100−2221−E−020−007−MY2, NSC−100−2221−E−020−005, and NSC−101−2221−E−020−021.

References

1. Y.C. Lin, T.H. Yu, C.F. Lin, *Chemosphere* 74 (2008) 131.
2. K. Choi, Y. Kim, J. Park, C.K. Park, M.Y. H.S. Kim, P. Kim, *Sci. Total. Environ*. 405 (2008) 120.
3. R. Andreozzi, M. Raffaele, P. Nicklas, *Chemosphere* 50 (2003) 139.
4. H. Nakata, K. Kannan, P.D. Jones, J.P. Giesy, *Chemosphere* 58 (2005) 759.
5. K.D. Brown, J. Kulis, B. Thomson, T.H. Chapman, D.B. Mawhinney, *Sci. Total. Environ*. 366 (2006) 772.
6. K.E. Murray, S.M. Thomas, A.A. Boduor, *Environ. Pollut*. 158 (2010) 3462.
7. S.F. Kang, C.H. Liao, M.C. Chen, *Chemosphere* 46 (2002) 923.
8. J.J. Pignatello, E. Oliveros, A. Mackay, *Crit. Rev. Environ. Sci. Technol*. 36 (2006) 1.
9. N. Masomboon, C. Ratanatamskul, M.C. Lu, *Environ. Sci. Technol*. 43 (2009) 8629.
10. N. Klamerth, K. Rizzo, S. Malato, M.I. Maldonado, A. Aguera, A.R. Fernandez-Alba, *Water Res*. 44 (2010) 545.
11. R. Andreozzi, V. Caprio, R. Marotta, D. Vogna, *Wat. Res*. 37 (2003) 992.
12. G. Chen, *Sep. Purif. Technol*. 38 (2004) 11.

13. C.A. Martinez-Huitle, S. Ferro, *Chem. Soc. Rev*. 35 (2006) 1324.
14. S. Balaji, S.J. Chung, R. Thiruvenkatachari, I.S. Moon, *Chem. Eng. J*. 126 (2007) 51.
15. M.E. Armenta-Armenta, A.F. Diaz, *Environ. Sci. Technol*. 39 (2005) 5872.
16. S. Balaji, V.V. Kokovkin, S.J. Chung, I.S. Moon, *Water Res*. 41 (2007) 1423.
17. M. Matheswaran, S. Balaji, S.J. Chung, I.S. Moon, *Chem. Eng. J*. 144 (2008) 28.
18. S. Balaji, S.J. Chung, M. Matheswaran, V.V. Kokovkin, I.S. Moon, *J. Hazard. Mater*. 150 (2008) 596.
19. A.M. Polcaro, S. Palmas, F. Renoldi, M. Mascia, *J. Appl. Electrochem*. 29 (1999) 147.
20. L. Gherardini, P.A. Michaud, M. Panizza, C. Comninellis, N. Vatistas, J. Electrochem. Soc. 148 (2001) D78.
21. Y. Samet, S. Chaabane Elaoud, S.Ammar, R.Abdelhedi, *J. Hazard. Mater*. B138 (2006) 614.
22. Y. Wei, B. Fang, T. Arai and M. Kumagai, *J. Appl. Electrochem*. 35 (2005) 561.
23. T. Raju, C. Ahmed Basha, *Chem. Eng. J*. 114 (2005) 55.
24. G. Li, J. Qu, , X. Zhang, J. Ge, *Water Res*. 40 (2011) 213.
25. Y. Zheng, W. Su, S. Chen, X. Wu, X. Chen, *Chem. Eng. J*. 174 (2011) 304.
26. D. Nematollahi, H. Shayani-Jam, M. Alimoradi, S. Niroomand, *Electrochim. Acta* 54 (2009) 7407.
27. Y. Li, S.M. Chen, *Int. J. Electrochem. Sci.* 7 (2012) 2175.
28. Y. Shen, F. Li, S. Li, D. Liu, L. Fan, Y. Zhang, *Int. J. Electrochem. Sci*. 7 (2012) 8702.
29. C. Bock, B. MacDougall, *J. Electrochem. Soc.* 146 (1999) 2925.
30. N.V. Smirnova, G.A. Tsirlina, S.N. Pron'kin, O.A. Petrii, *Russ. J. Electrochem.* 35 (1999) 113.
31. C. Terashima, T.N. Rao, B.V. Sarada, D.A. Tryk, A. Fujishima, *Analytical Chemistry* 74 (2002) 895.
32. Y.H. Cui, J. X.Y. Li, G. Chen, *Water Res*. 43 (2009) 1968.
33. M. Murugananthan, S. Yoshihara, T. Rakuma, T. Shirakashi, *J. Hazard. Mater*. 154 (2008) 213.
34. G.F. Pereira, R.C. Rocha-Filho, N, Bocchi, S.R. Biaggio, *Chem. Eng. J*. 198 (2012) 282.
35. M. Matheswaran, S. Balaji, S.J. Chung, I.S. Moon, *Chemosphere* 69 (2007) 325.
36. T.S. Chen, K.L. Huang, Y.C. Lai, Y.M. Kuo, *J. Environ. Manage*. 104 (2012) 85.

© 2012 by ESG (www.electrochemsci.org)